TELFER'S GEOSIM METHOD REVISITED BY CFD

(DOI No: 10.3940/rina.ijme.2019.a4.563)

C Delen and **S Bal**, Department of Naval Architecture and Marine Engineering, Istanbul Technical University, Turkey

SUMMARY

In this study, Telfer's GEOSIM method for the computation of ship resistance at full scale has been applied by CFD (Computational Fluid Dynamics) approach. For this purpose, the KCS (KRISO Container Ship) hull has been investigated numerically with k-ε turbulence model for three different scales and full scale analyses by URANS (Unsteady Reynolds Averaged Navier-Stokes) method. Full scale ship resistance has been predicted using the numerical results computed at different model scales by Telfer's GEOSIM method. The numerical results at three scales have also been extrapolated separately to that at full scale by ITTC 1978 performance prediction method. An experimental study has also been carried out at a model scale for validation. The results by Telfer's GEOSIM method have been calculated almost in full compliance with those of CFD approach. While the difference between the results of CFD and those of ITTC extrapolation method is about 5% at full scale, the difference between the results of CFD and those of Telfer's GEOSIM method has been found to be less than 1% at full scale. In addition, this method has been applied to estimate the nominal wake coefficient at full scale from model scales. A very good correlation has also been found for nominal wake coefficient.

NOMENCLATURE

B	Breadth (m)
C_A	Correction allowance
C_{AA}	Air resistance coefficient
C_R	Residual resistance coefficient
C_B	Block coefficient
C_F	Frictional resistance coefficient
CFD	Computational Fluid Dynamics
C_T	Total resistance coefficient
e_{ext}	Extrapolated relative error
e_a	Approximate relative error
EFD	Experimental Fluid Dynamics
Fr	Froude number
FVM	Finite Volume Method
g	Acceleration of gravity (m s^{-2})
GCI	Grid Convergence Index
GEOSIM	Geometrically similar
ITTC	International Towing Tank Conference
k	Form factor
KCS	KRISO container ship
L_{BP}	Length between perpendiculars (m)
LCB	Longitudinal Center of Buoyancy (m)
L_{WL}	Length on waterline (m)
N/A	Not available
N_i	Total mesh number of i^{th} grid
p	Apparent order of method
R	Converged condition
r	Refinement factor
Re	Reynolds number
R_T	Hull resistance (N)
S	Wetted surface area (m^2)
SIMPLE	Semi-Implicit Method for Pressure-Linked Equations
Subscript_M	Model scale
Subscript_S	Full scale
T	Draught (m)
U_D	Uncertainty value in experiments.
U_{GCI}	Uncertainty value in simulation.
U_V	Validation Uncertainty
URANS	Unsteady Reynolds Averaged Navier-Stokes
V	Service speed (m s^{-1})
V&V	Verification and validation
w_n	Nominal wake fraction
∇	Displacement volume (m^3)
ΔC_F	Roughness allowance
Δt	Time step (s)
ʎ	Scale ratio
ρ	Density of fluid (kg m^{-3})
σ	Sinkage (m)
τ	Trim (°)
υ	Kinematic viscosity (m^2 s^{-1})
ϕ_i	Solution of key parameter of i^{th} grid

1. INTRODUCTION

One of the main issues in the design of a marine vessel is the correct estimation of power required at the desired velocity. Overestimation of power would cause an increase in production and operational costs as well as in emissions from ship. On the other hand, underestimation of power would cause not to satisfy the operational criteria of the vessels. For this purpose, the vessel resistance and power at a desired speed should be determined precisely.

Telfer's GEOSIM method is one of the significant methods to estimate the ship resistance and power at full scale by using model tests. Total resistance is predicted without theoretical decomposition of resistance (Bertram, 2011). This method, unlike other conventional methods, provides an extrapolating technique to full scale by using only total resistance values at model scales (Molland *et al.*, 2011). The main purpose in original Telfer's GEOSIM method is to determine a relationship between the total resistance of the ship and the Reynolds number by carrying out model tests with geometrically similar (GEOSIM) models at corresponding Froude numbers (Telfer, 1927). However, carrying out model experiments with a series of model family is both time consuming and

expensive. Kinematic similarities can also be violated during tests due to the effects of tank side walls particularly for large models and occurrence of much laminar flow near bow section of small models. Estimation of resistance from model scale to full scale can lead to inaccuracies, especially in high Reynolds numbers. Due to such major disadvantages, this method has not been preferred much to determine the total resistance of ships at full scale. But now CFD and numerical towing tank applications have been widely used. The solution to ship resistance problem has been facilitated using developed processing capability and CFD applications for both model families and ships at full scale. Many features of a hull can be investigated in processing and post-processing stages both numerically and visually by CFD methods. Here original Telfer's GEOSIM method has been revisited by using CFD applications

CFD method has widely been used to solve the ship hydrodynamic problems. Shen *et al.* (2015) have simulated towed tests of KCS, open water tests of the KP505 propeller, self-propulsion and zig-zag manoeuvres of KCS model to validate the dynamic overset grid technique. Gaggero *et al.* (2015) have showed that the hydrodynamic properties of KCS hull could successfully be investigated with OpenFOAM RANS solver. Ozdemir *et al.* (2016) have investigated the capability of a CFD code on KCS hull. Numerical results have been compared with the available experiment data. In the study of De Luca *et al.* (2016), a comprehensive V&V study was conducted to assess the reliability of URANS simulations of a planing hull. RANS based CFD approach was applied for wave resistance problem of ships in Kinaci *et al.* (2016). They also examined the dependency of form factor to Reynolds number. Self-propulsion points of KCS hull have been obtained with the methods based on CFD approach in Kinaci *et al.*, (2018). They have also proposed a simple method for predicting self-propulsion points of marine vehicles using some empirical relations. Gokce *et al.* (2018) have predicted hydrodynamic characteristics of Japan Bulk Carrier (JBC) using RANS method. Numerical results have been compared with empirical relations recommended by International Maritime Organization (IMO). The numerical results have been found more robust than IMO recommendations. Sezen *et al.* (2018) have examined the hydrodynamic properties of a submerged body in a wide velocity range by RANS approach.

In the past GEOSIM series have generally been used to study the scale effects on the form factor, e.g., García-Gómez (2000); Lin and Kouh (2015); Srinakaew (2017). For example, Kouh *et al.* (2009) have numerically investigated the scale effect on form factor. Four surface ship and two sub-bodies have been simulated with double-model flow in a wide range of Re numbers. The difference between these studies and this study is that only one scale of each hull was performed with different Re numbers. In present study computations have been carried out at different scale ratios. Flow interference phenomena between catamaran hulls has also been examined numerically with GEOSIM approach in Broglia *et al.* (2011). In contrast to these studies, GEOSIM model series have been applied to estimate the total resistance of full scale ships in the present study.

CFD methods can also be used to solve the complex flow problem around hull forms not only at model-scale but also at full scale. In study of Castro *et al.* (2011) resistance and self-propulsion simulations of the KCS hull at full scale have been carried out numerically. The coefficients obtained from CFD have been compared and discussed with the results from ITTC extrapolation procedures. Tezdogan *et al.* (2015) have predicted ship motions and added resistance of a full scale KCS hull with fully nonlinear unsteady RANS method. The results have been validated with available experimental data and also compared with those of potential flow theory. Park *et al.* (2015) have proposed a new method for the propulsive performance prediction at full scale, including the effect of an energy saving device (ESD). Free surface effect has not taken into account in full scale CFD analysis. Lin and Kouh (2015) have performed a numerical resistance test, open water performance and self-propulsion tests at different scales of KCS hull without considering free water surface effects. As a result of the study, the scale effect on thrust deduction has been discussed and compared to the conventional standard ITTC procedure. Haase *et al.* (2016) has proposed a novel CFD-based approach to predict the resistance at full scale. For both model and full scale CFD simulations, model tests and sea trials have been used for an agreement of resistance with established model-ship correlation lines and surface roughness effects. In another study of Tezdogan *et al.* (2016), the seakeeping behaviour of a full scale large tanker and its heave and pitch responses to head waves hull have been investigated at various water depths. Numerical results have been reported to be consistent with the experimental results and the results from 3D potential theory. In the paper of Jasak *et al.* (2018), full scale CFD self-propulsion has been compared with sea trials for two types of ships: a general cargo and a car carrier. The results obtained from full scale open water propeller tests have been used as an input in self-propulsion with the actuator disc model. Song *et al.* (2019) have examined the effect of barnacle fouling on the resistance and wake characteristics of full scale KCS hull. The roughness function has been validated with model-scale flat plate simulation then this approach has been employed in full scale flat plate simulation and full scale 3D KCS hull simulations.

In the present study, the total resistance of a full scale ship has been predicted using Telfer's GEOSIM method (Telfer, 1927) based on CFD approach. The model tests of the KCS hull at 60.75 scale ratio were also conducted in the Ata Nutku Ship Model Testing Laboratory of Istanbul Technical University. Numerical analysis of KCS hull at three different model scales and full scale have been carried out by the fully nonlinear unsteady RANS method. In order to determine the grid independence of the numerical model, a spatial convergence study has been

conducted with Grid Convergence Study (GCI) method for KCS hull at a sample scale ratio. The numerical results obtained for three scales have been validated with the experiments carried out at Istanbul Technical University and available data in the literature. The relationship between total resistance coefficient and Re number has been correlated by Telfer's GEOSIM method. The results computed by Telfer's GEOSIM method have been found to be less than 1% at full scale ship while the results obtained by ITTC extrapolation method have been found to be larger than those of Telfer's GEOSIM method. Additionally, Telfer's GEOSIM method has then been extended to the computation of nominal wake at full scale by using wake values at three different model scale ratios. A good correlation has also been found for nominal wake values.

2. METHODOLOGY

2.1 NUMERICAL MODEL

Three dimensional unsteady Reynolds Averaged Navier-Stokes (RANS) equation for incompressible flow along with continuity equation are given below.

$$\frac{\partial U_i}{\partial x_i} = 0 \tag{1}$$

$$\frac{\partial U_i}{\partial t} + \frac{\partial U_j U_i}{\partial x_j} = -\frac{1}{\rho}\frac{\partial P}{\partial x_i} + \frac{\partial(-\overline{u_i' u_j'})}{\partial x_j} + \nu\frac{\partial^2 U_i}{\partial x_j^2} \tag{2}$$

Here U_i is the mean velocity in the i^{th} direction of the Cartesian coordinate; ρ is the density, P is the mean pressure, $\overline{u_i' u_j'}$ is the Reynolds stress and ν the kinematic viscosity. In the present study, two equation k-ε turbulence model is used for modelling the Reynolds stress(τ_{ij}) . In standard k-ε model, the Reynolds stress is related to strain rate linearly as follows:

$$\tau_{ij} = \overline{u_i' u_j'} = \frac{2}{3}k\delta_{ik} - \nu_t\left(\frac{\partial U_i}{\partial x_i} + \frac{\partial U_j}{\partial x_i}\right) \tag{3}$$

where ν_t represents the eddy kinematic viscosity ($\nu_t = C_\mu {k^2}/{\epsilon}$). C_μ is an empirical constant and its value is equal to 0.09. The turbulence kinetic energy (k) and its rate of dissipation (ε) are obtained from the following transport equations.

$$\frac{Dk}{Dt} = -\overline{u_i' u_j'}\frac{\partial U_i}{\partial x_i} - \varepsilon + \frac{\partial}{\partial x_j}\left[\left(\frac{\nu_t}{\sigma_k} + \nu\right)\frac{\partial k}{\partial x_j}\right] \tag{4}$$

$$\frac{D\varepsilon}{Dt} = -C_{\varepsilon 1}\frac{\varepsilon}{k}\overline{u_i' u_j'}\frac{\partial U_i}{\partial x_i} - C_{\varepsilon 2}\frac{\varepsilon^2}{k} + \frac{\partial}{\partial x_j}\left[\left(\frac{\nu_t}{\sigma_k} + \nu\right)\frac{\partial \varepsilon}{\partial x_j}\right] \tag{5}$$

In these equations, $C_{\varepsilon 1} = 1.44$ and $C_{\varepsilon 2} = 1.92$ are constant, $\sigma_k = 1.0$ and $\sigma_\varepsilon = 1.3$ are turbulent Prandtl numbers for k and ε (Jones and Launder, 1972)

2.2 TELFER'S GEOSIM METHOD

As it is known, resistance coefficient of geometrically similar hulls is based on Froude and Reynolds numbers analogy. The non-dimensional resistance coefficient of a hull can be expressed as:

$$\frac{R}{\rho S V^2} = f\left(\frac{V}{\sqrt{gL}}, \frac{\upsilon}{VL}\right) \tag{6}$$

Here the first term in the parenthesis of functional expression is Froude (Fr) number and represents gravity wave resistance, the second term is Reynolds (Re) number and represents viscous resistance. The extrapolation of viscous phenomena from model scale to largest conceivable ship has been expressed as 1/Re since viscous forces have not significant contribution in higher Re numbers (Telfer, 1927). In Telfer' s GEOSIM method, the total resistance of a ship is expressed as a function of Re number, using geometrically similar models. Since the Fr number is the same in the model scale and the full scale, the inertia (residual) resistance coefficient is assumed to be the same for both model and ship. The non-dimensional resistance values (C_T) are then plotted against a wide range of Re numbers of the model family. Finally, the model resistance can be extrapolated to full scale resistance by C_T-Re curve. The curve of ship resistance versus Re number can be expressed as;

$$C_T = \frac{a}{(log\ Re)^x} + b \tag{7}$$

In this equation, power x is generally taken as 1/3, then a linear system of two equations with two unknowns (a and b) is solved. However, in this study, power x has also been assumed to be an unknown parameter to increase the accuracy of Telfer's GEOSIM method, especially in high Re number. Three unknowns (a, b and x) can be solved by resistance values at three different model scales for a corresponding Fr number. Equation 7 generates a nonlinear system which can be solved by a least square method (Nocedal and Wright, 2006).

2.3 1978 ITTC PERFORMANCE PREDICTION METHOD

The results of ITTC 1978 method were compared with those of Telfer's GEOSIM method. The total resistance coefficient of a ship without bilge keel can be given as,

$$C_{TS} = (1+k)C_{FS} + \Delta C_F + C_A + C_{AAS} + C_R \tag{8}$$

where *(1+k)* is the form factor by Prohaska, C_{FS} is the frictional resistance coefficient of the ship according to the ITTC-1957 model-ship correlation line, ΔC_F is the roughness allowance, C_A is the correction allowance, C_{AAS} is the air resistance coefficient, C_R is the residual resistance coefficient that is considered as the same value for both the model and full scale ship (ITTC, 2011a). C_R is calculated as follows (ITTC, 2011c):

$$C_R = C_{TM} - (1+k)C_{FM} \tag{9}$$

Here, C_{TM} can be expressed in non-dimensional form by resistance measured of model,

$$C_{TM} = \frac{R_{TM}}{0.5\rho_M S_M V_M^2} \tag{10}$$

C_{FM} is calculated with Re number by ITTC-1957 line as follow,

$$C_{FM} = \frac{0.075}{(\log Re_M - 2)^2} \tag{11}$$

The form factor can be calculated by (ITTC, 2011c). In this study, only two main resistance components, C_F and C_R have been considered. Detailed information about other coefficients and calculations can be found at ITTC, (2011b, 2011a).

3. GEOMETRY AND TEST CASES

In this study, a modern container ship (KCS) has been selected for the CFD analysis. KCS has a bulbous bow designed by Korea Research Institute of Ships and Ocean Engineering (Van *et al.*, 1998; Kim *et al.*, 2001). KCS hull is widely used for validation & verification of CFD applications (Carrica *et al.*, 2010; Simonsen *et al.*, 2013; Gaggero *et al.*, 2017). The main dimensions of the model families of KCS used in this study, have been given in Table 1. The general views of the KCS model have been shown for Model 1 in Figure 1.

These scale ratios used in this study have been selected since they are frequently used in the literature. The experiments of Model 1 were also carried out in Ata Nutku Ship Model Testing Laboratory of Istanbul Technical University (Delen and Bal, 2015a). The model tests of Model 2 and Model 3 (other scales) were performed in FORCE and NMRI towing tanks, respectively. Model 2 and 3 are also one of the benchmark cases (cases 2.1 & 2.10) in Tokyo 2015 Workshop on CFD in ship hydrodynamics. The CFD analyses of KCS hulls with rudder were carried out in calm water at design Fr number as in the experimental conditions.

Table 1: Main particulars of KCS.

Parameter	Model 1	Model 2	Model 3	Full scale
λ	60.75	37.89	31.6	1.0
L_{PP} (m)	3.786	6.070	7.278	230.0
B (m)	0.530	0.850	1.019	32.2
T (m)	0.178	0.285	0.342	10.8
S (m^2) (w/rudder)	2.585	6.644	9.553	9539
∇ (m^3)	0.232	0.956	1.649	52030
C_B	0.643			
LCB (%L_{PP}), fwd+	-1.48			
V (m/s)	1.584	2.006	2.196	12.346
Fr	0.26			
Re	5.26E+06	1.07E+07	1.40E+07	2.49E+09

Figure 1: Views of KCS hull (Model 1).

4. EXPERIMENTAL SETUP

KCS model was produced in accordance with the ITTC (2011c) Recommendation Procedures and Guidelines at 60.75 scale ratio in the laboratory workshop in 2014. Resistance tests of KCS hull were conducted in the towing tank of Ata Nutku Ship Model Testing Laboratory. The towing tank has a length of 160 m, a width of 6 m, a water depth of 3.5 m. The maximum speed of the towing carriage is 5.5 m/s. Uncertainty analysis of resistance tests had also been estimated for this model with ITTC, (2002) and ITTC, (2014). For this study, the experiments have been extended to include the trim values of Model 1 into results. The resistance, trim and velocity signals have been measured simultaneously by taking into account the ITTC procedures (ITTC, 2002a, 2011a, 2011c). Tested model had a certain freedom of movement (sinkage and trim) during tests. The measurement data have been processed considering the same time domain. The expanded uncertainty value of total resistance coefficient of KCS

hull in this towing tank has been estimated as ± 1.16% according to ITTC (2014b) method for Fr=0.26 (Delen and Bal, 2015b). In this study, the experimental results have been used only for validation. A profile view of KCS at the Fr=0.26 has been shown in Figure 2.

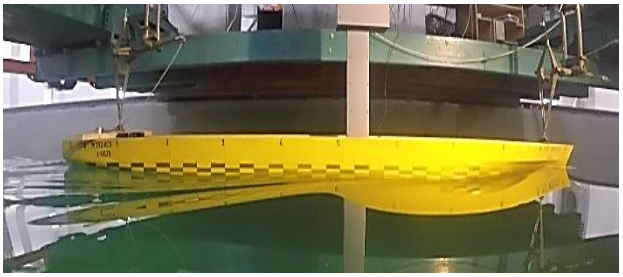

Figure 2. A profile view of Model 1 at Fr = 0.26.

5. NUMERICAL SETUP

5.1 COMPUTATIONAL DOMAIN AND BOUNDARY CONDITIONS

Dimensions of computational domain ($-1 \leq x/L_{PP} \leq 3$, $0 \leq y/L_{PP} \leq 2$, $-1.5 \leq z/L_{PP} \leq 0.5$) have been selected to take into account ITTC (2011b) recommendations and to avoid any influence on the wave pattern. The Cartesian coordinate system was adopted in the CFD analysis. The origin of coordinate system is at the point where fore perpendicular intersects the waterline. The positive x-, y-, z- axes have been defined as in the stream-wise, starboard and upward directions, respectively. In order to reduce the computational time, half of the hull (only starboard side) has been used in the analysis. The centreline of KCS hull has been defined as the symmetry plane. The upstream and surrounding boundaries have been defined as velocity inlet to impose Dirichlet type of boundary condition. This boundary condition is very suitable for the incompressible flows, in which the velocity profile is known at inlet boundary. The downstream boundary has been defined as pressure outlet (gradient normal to the boundary of velocity) by Neumann boundary condition. No-slip kinematic boundary condition has been adopted on the hull surface. Detailed information on the boundary conditions can be found in the user guide of CD-adapco (2017). Computational domain and boundary conditions have been shown in Figure 3.

5.2 GRID STRUCTURE

Computational domain has been created by the overset mesh technique due to the large amplitude motions of form (especially in full scale condition). There should be a good overlap between the background and the overset grids in order to represent the flow accurately around the hull form. The dimensions of overset domain have been taken as $-0.12 \leq x/L_{PP} \leq 1.12$, $0 \leq y/L_{PP} \leq 0.12$ and $-0.12 \leq z/L_{PP} \leq 0.12$. The computational domains have been divided into unstructured hexahedral cells. The mesh structure has been refined in terms of cell size, especially on free surface and in the wake region. The total numbers of mesh for Model 1, Model 2, Model 3 and full scale ship are 1.89, 2.41, 2.52, 11.5 million, respectively. Mesh structure along the centreline of KCS can be seen for Model 1 in Figure 4.

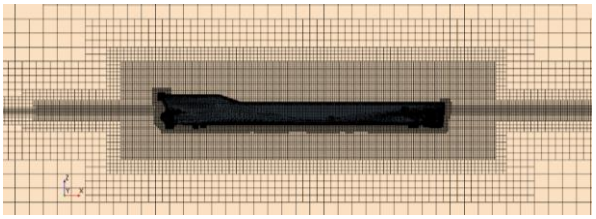

Figure 4. Grid structure of KCS (Model 1).

5.3 SOLUTION STRATEGY

The governing equations have been discretized using a cell based finite volume method (FVM). SIMPLE (Semi-Implicit Method for Pressure-Linked Equations) algorithm which allows to couple the Navier-Stokes equations with an iterative procedure has been used to solve the pressure field. The flow around the hulls has been considered fully turbulent, 3-D and multiphase. To simulate the flow around the hull, the k-ε turbulence model has been selected. Quérard *et al.* (2008) reported that the k-ε model is more economical in terms of CPU execution time than k-ω turbulence model.

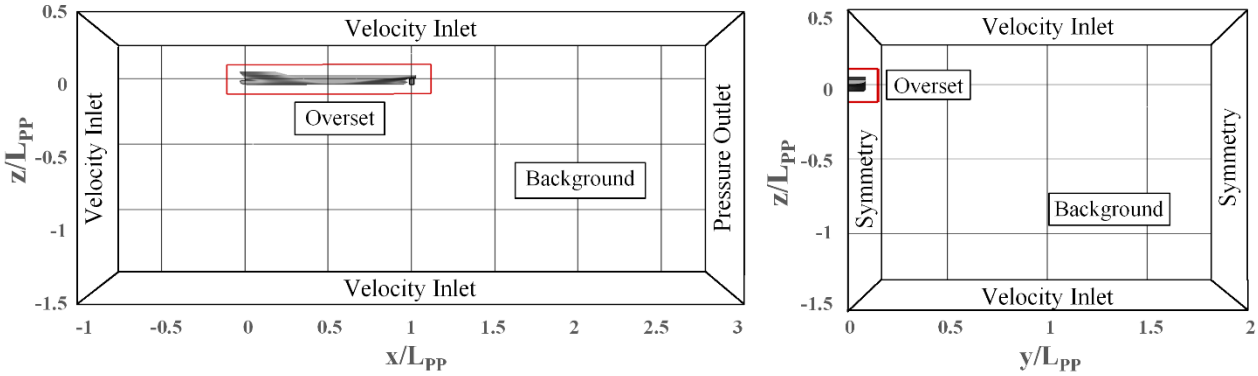

Figure 3. Profile and side views of the computational domain with boundary conditions.

There are also some other studies in the literature that k-ε model has been applied to simulate the turbulent flow, such as, Cakici *et al.* (2017), Delen *et al.* (2017), Terziev *et al.*, (2018). In order to represent the surface gravity waves on the interface between the heavy fluid and light fluid, the Volume of Fluid (VOF) method has been chosen in this study. The VOF method is a suitable method both for tracking the free surface between immiscible fluids and for capturing a high-resolution interface (CD-adapco, 2017). A second order convection scheme has been preferred to capture the surface interfaces between the two phases quite well. The phases are chosen as fresh water and air. The temperature of fluids is set to 15ºC (ρ_{water}=999.1 kg/m^3, ν_{water}=1.14E-06 m^2/s). The calm water condition has been defined by the flat VOF wave. In order to avoid wave reflections on free surface from the surrounding boundaries of computational domain, the VOF wave damping model has been activated far enough away from hull. The coupling between fluid and body has been established with the Dynamic Fluid-Body Interaction (DFBI). The DFBI provides the motion of the form, taking into account the balance of forces and moments at the boundary. In CFD simulations, the motion of hull has been set to free to trim and sinkage. The time step (Δt) in numerical analyses has been determined as $\Delta t = 0.005\,L/U$ recommended by ITTC (2011b) for each model. Detailed information on the solution strategy are given in the user guide of CD-adapco (2017). The wall y$^+$ values for the underwater surfaces of models are around 100 for each hull. A sample image of wall y$^+$ contour has been shown for model 1 in Figure 5.

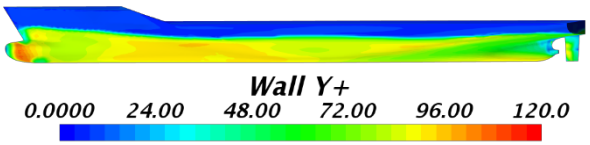

Figure 5. Wall y$^+$ distributions on the model 1 surface at Fr=0.26.

6. V&V STUDY

A verification study has been conducted on the numerical model in terms of grid size to estimate numerical uncertainty. GCI method which is frequently used in CFD applications, has been used to determine the appropriate mesh structure, e.g., De Marco *et al.* (2017), Dogrul *et al.* (2017), Usta and Korkut (2018). In this study, the total resistance coefficient has been selected as key parameter. Since the estimation of uncertainty of grid structure for each model would require a lot of solution time, the uncertainty study has been conducted only for Model 1. For the other models, grid size of the hull surface and free surface region have been refined systematically.

GCI method has been briefly described as follows. $\varepsilon_{32} = \phi_3 - \phi_2$ & $\varepsilon_{21} = \phi_2 - \phi_1$, ϕ_i represent the solution of key parameter of ith grid. The convergence condition ($R = \varepsilon_{21}/\varepsilon_{32}$) must be examined. If the R value is between 0 and 1, the solution of numerical model converges monotonically (Stern *et al.*, 2002). This means that numerical uncertainty can be estimated quantitatively by the GCI method. The apparent order of method (p) is calculated by,

$$p = \frac{1}{\ln(r_{21})}\left|\ln\left|\varepsilon_{32}/\varepsilon_{21}\right| + q(p)\right| \tag{12}$$

$$q(p) = \ln\left(\frac{r_{21}^p - s}{r_{32}^p - s}\right) \tag{13}$$

$$s = \begin{Bmatrix} -1 & if & \varepsilon_{32}/\varepsilon_{21} < 0 \\ +1 & if & \varepsilon_{32}/\varepsilon_{21} > 0 \end{Bmatrix} \tag{14}$$

where, r_{21} and r_{32} are refinement factor calculated by $r_{21} = \sqrt[3]{N_1/N_2}$, $r_{32} = \sqrt[3]{N_2/N_3}$. It is recommended that refinement factor greater than 1.3 (Celik *et al.*, 2008). N_i denotes the mesh number of ith grid. The extrapolated value is calculated by,

$$\phi_{ext}^{21} = \frac{r_{21}^p \phi_1 - \phi_2}{r_{21}^p - 1} \tag{15}$$

The approximate relative error can be expressed as follows:

$$e_a^{21} = \left|\frac{\phi_1 - \phi_2}{\phi_1}\right| \tag{16}$$

Then, the relative error can be obtained by,

$$e_{ext}^{21} = \left|\frac{\phi_{ext}^{21} - \phi_1}{\phi_{ext}^{21}}\right| \tag{17}$$

The fine-grid convergence index is estimated by,

$$GCI_{fine}^{21} = \frac{1.25 e_a^{21}}{r_{21}^p - 1} \tag{18}$$

Detailed information of GCI method can be found in (Celik *et al.*, 2008). Three significantly different sets of grids, called fine, medium and course, corresponding to cell numbers N_1, N_2 and N_3, have been generated. The analyses have been simulated to examine the change of key parameter (C_T). The converged condition (R) value has been found as 0.262. The other coefficients of GCI method have been given in Table 2. As a result, the numerical uncertainty of fine grid has been estimated as 1.06% and fine grid type has been then selected for rest of analyses.

Table 2. Coefficients of discretization error of Model 1.

N_1, N_2, N_3	1.91E+06, 8.31E+05, 3.73E+05
ϕ_1, ϕ_2, ϕ_3	4.37E-03, 4.35E-03, 4.26E-03
r_{21}, r_{32}	1.32, 1.31
p	4.999
q(p)	4.66E-02
ϕ_{ext}^{21}	4.38E-03
e_a^{21}	0.025
e_{ext}^{21}	0.17%
GCI_{fine}^{21}	1.06%

Validation uncertainty (U_V) by combining experimental and numerical uncertainty can be expressed as follows (Stern *et al.*, 2002; De Luca *et al.*, 2016).

$$U_V^2 = U_D^2 + U_{GCI}^2 \quad (19)$$

In this calculation only grid-spacing converge error (U_{GCI}) has been taken into consideration. U_D is the uncertainty that occurs in the experiment. U_D was calculated as ±1.16%. Detailed information about U_D can be found in (Delen and Bal, 2015b). U_V has been calculated as ± 1.57%. Finally, validation has been achieved because the absolute relative difference between the numerical result and the experiment (|% ΔC_T| = 1.33%) has been found below the U_V. Actually, other sources of uncertainty (e.g., iterative convergence error and time-step convergence error etc.) are also recommended to be included in the calculation. However, when these error components are included, U_V value will increase and there will be no negative effect on validation of solution. Therefore, it has not been included in this study.

7. RESULTS AND DISCUSSION

Numerical resistance coefficient (C_T), sinkage (σ) and trim (τ) values have been compared with available experimental data in Table 3. The relative difference between the results of CFD and EFD has been calculated by $\Delta\%CFD = 100 \times |CFD - EFD|/EFD$). There is a good agreement between the results (C_T, σ and τ) of CFD and EFD methods. In the study of Castro *et al.* (2011) resistance of the KCS hull at full scale without rudder effect has been computed. The resistance is found to be approximately 4.5% higher than that of the smooth wall surface. The reason for this difference between the two studies is the effect of rudder.

In order to validate the numerical method, the wave elevations at y/L_{PP}=0.1509 have been shown for each model in Figure 6. The agreement between models is very satisfactory. The wave profiles on hull surface have also been plotted in Figure 7. Since the wave profiles on hull surface have not predominantly been affected by viscosity, the wave profiles of the models and of the full scale ship have been consistent with each other. Wave patterns on the free surface have also shown in Figure 8 for each model. Wave heights are compatible with each other.

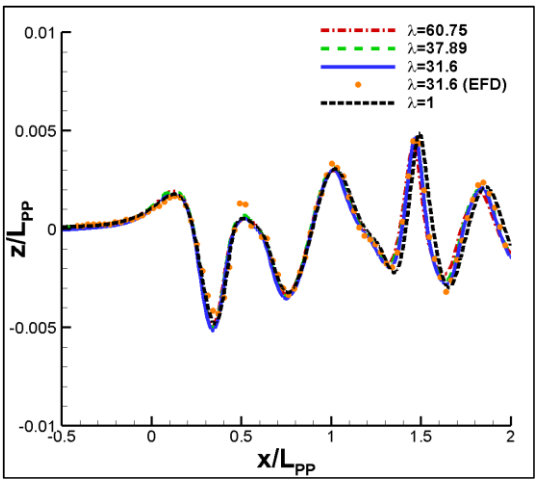

Figure 6. Wave profile along the y/L_{PP}=0.1509.

Nominal wake coefficients of models and of full scale hull have been given in Table 4. Due to viscous effects, the wake of hull at full scale has been found quite different than that of hull at λ=31.6 scale ratio. Nominal wake distributions at x/L_{PP}=0.9825 have been given in Figure 9 for GEOSIM models and full scale as recommended by ITTC (2014c).

Table 3. Comparison of EFD and CFD results at Fr=0.26.

λ	$C_T \times 10^3$			$\sigma \times 10^2$ (m)			τ (degree)		
	EFD	**CFD**	**% ΔC_T**	**EFD**	**CFD**	**% Δσ**	**EFD**	**CFD**	**% Δτ**
60.75	4.430*	4.371	1.33%	N/A	-0.722	-	-0.161	-0.164	1.57%
37.89 (Larsson *et al.*, 2018)	3.835	3.938	2.68%	-1.259	-1.180	6.28%	-0.165	-0.167	1.73%
31.6 (Larsson, *et al.*, 2013)	3.659**	3.793	3.67%	-1.394	-1.399	0.39%	-0.169	-0.165	2.33%
1	N/A	2.294	-	N/A	-42.664	-	N/A	-0.151	-

* Delen and Bal (2015b).
**Measured resistance value has been modified to 15 ºC by ITTC (2014a).

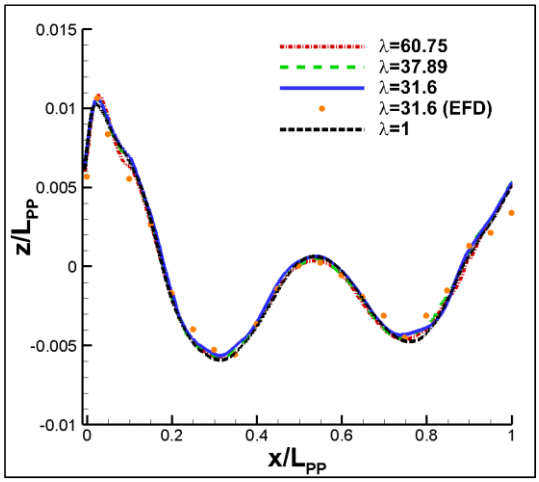

Figure 7. Wave profile on hull

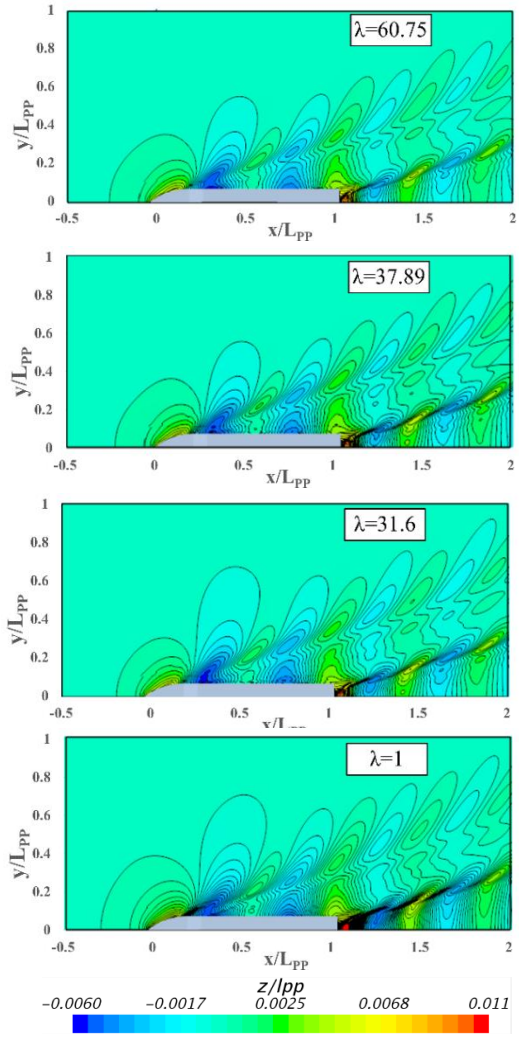

Figure 8. Wave patterns on free surface for Fr=0.26.

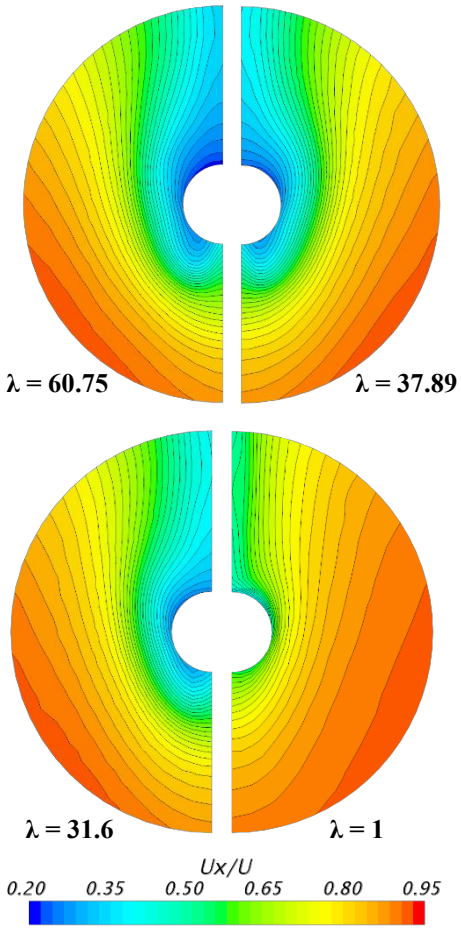

Figure 9. Nominal wake contours by CFD for x/LPP=0.9825.

Table 4. Nominal wake coefficients at x/L_{PP}=0.9825

λ	EFD	CFD	
	$1-w_n$	$1- w_n$	% $\Delta(1- w_n)$
60.75		0.671	3.93%
37.89		0.699	0.21%
31.6	0.698	0.709	1.53%
1		0.816	16.86%

The workstation PC used for the solution of numerical analysis has a 64-bit 2.2 GHz-2 processors, 88 cores (44 of them are logical cores) and 256 GB RAM. The CPU execution times of models 1,2, 3 and full scale are 12.33 hours, 13.34 hours, 14.72 hours, and 110 hours for this PC, respectively. Estimation of full scale results by model tests is much economical than that of full scale solutions.

Coefficients (a, b and x) of Eq. 7 have been calculated as 2.3202, $1.3767*10^{-3}$ and 3.4917, respectively, at full scale for total resistance coefficient of KCS hull. Full scale results of KCS obtained by ITTC 1978 have also been shown in Table 5. Form factor (1+k) has been taken as 1.1 in all processes since ITTC-1957 correlation line had

already a form factor correction (ITTC, 2011c). All estimated results (by Telfer and ITTC methods) have been compared with those of CFD method at full scale as shown in the Table 5. Relative difference (between the resistance of Telfer's GEOSIM method (TGM) and that of CFD ($\Delta\%C_{TS} = 100 \times |C_{TS-TGM} - C_{TS-CFD}|/C_{TS-CFD}$) is less than that of ITTC 1978 method and CFD ($\Delta\%C_{TS} = 100 \times |C_{TS-ITTC} - C_{TS-CFD}|/C_{TS-CFD}$). This is very clear in Table 5. The numerical resistance values and extrapolated results by both Telfer's GEOSIM method and ITTC method have been shown in the Figure 10. Resistance value at full scale by Telfer's GEOSIM method is closer to that by CFD than resistance value calculated by ITTC 1978 method. This can be due to not decomposition of total resistance into components by Telfer's method.

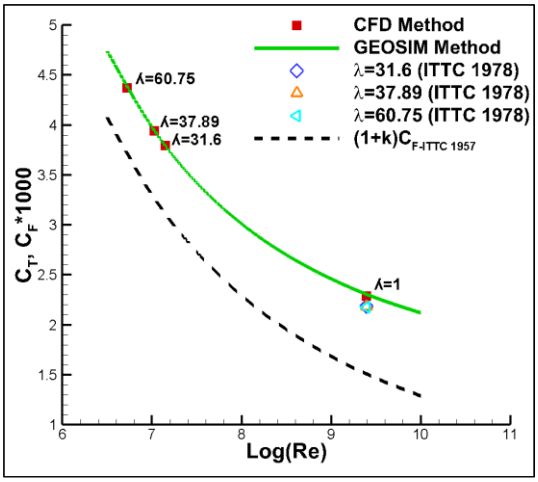

Figure 10. Comparison of total resistance coefficients.

Telfer's GEOIM method has also been extended to the prediction of wake fraction of ship at full scale. Coefficients (a, b and x) have been calculated as -93.291, 0.885 and 3.191, respectively, for the full scale nominal wake fraction. Wake scaling has been successfully represented by the Telfer's GEOSIM method as given in Table 5. Relative difference between the wake fraction by Telfer's GEOSIM method (TGM) and that of CFD ($\Delta\%(1-w_n) = 100 \times |(1-w_n)_{TGM} - (1-w_n)_{CFD}|/(1-w_n)_{CFD}$) has been found to be less than 1%. Wang *et al.* (2015) had previously proposed a method with a relationship between the nominal wake and Re number similar to this method. However, in this study, the exponential force of *log(Re)* has also been calculated to represent the slope of the curve much better as shown in the total resistance coefficient curve (Figure 11).

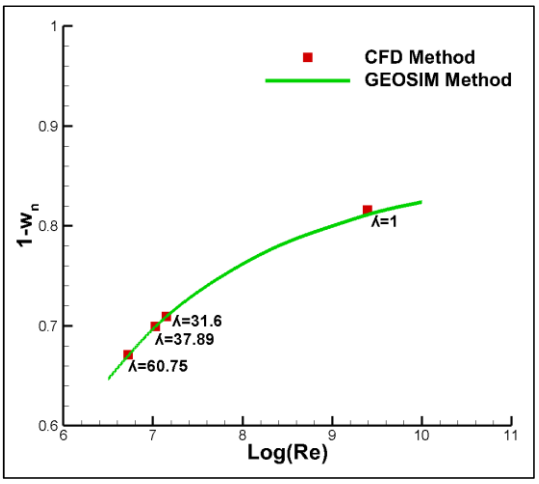

Figure 11. Comparison of nominal wake fractions by different method

8. CONCLUSION

In this study GEOSIM method of Telfer has been applied to compute the ship total resistance coefficient and nominal wake fraction at full scale by CFD analysis. KCS hull has been selected to validate the results. Numerical results of models at three scale ratios have been compared and validated with those of experimental data. Full scale resistance analysis of KCS hull has also been performed numerically. The extrapolated full scale results (GEOSIM method and ITTC 1978 method) have been compared with those of CFD analyses. Resistance values extrapolated by ITTC 1978 method have been found about 5% smaller than that of CFD at full scale. This difference is less than 1% by the Telfer's method. It has been found that Telfer's GEOSIM method in a wide range of Re numbers can be successfully used with the help of the numerical models at three scales. There is no need to decompose the resistance components and to solve ship flow problem at full scale which requires too much computational time.

This method has also been extended to the estimation of nominal wake fraction in a way similar to total resistance coefficient. The estimated nominal wake value has also been found in a good agreement with that of CFD analyses.

Table 5. Comparison of full scale resistance methods for KCS at Fr = 0.26.

	CFD Method	Telfer's GEOSIM Method	ITTC 1978 Method		
			λ=60.75	λ=37.89	λ=31.6
$C_{TS}*10^3$	2.294	2.306	2.177	2.183	2.186
$\%\Delta C_{TS}$	-	**0.53%**	**5.08%**	**4.86%**	**4.70%**
$1-w_n$	0.816	0.811			
$\%\ \Delta(1-w_n)$	-	**0.53%**			

9. ACKNOWLEDGEMENTS

This study is dedicated to commemorating the distinguished Prof E.V Telfer who was the founder of the branch of Naval Architecture of Istanbul Technical University (Baykal, 2015). He was also the first chairperson of this branch between 1946-1951 (Walker, 2010) and the first professor of Naval Architecture in Istanbul, Turkey (RINA, 1977).

This research was supported by the Coordination Unit of Scientific Research Projects of Istanbul Technical University (Project number: MGA-2017-40961).

10. REFERENCES

1. BAYKAL, R. (2015) *History of Naval Architecture and Ocean Engineering in Turkey*. Istanbul: ITU Foundation Press.
2. BERTRAM, V. (2011) *Practical ship hydrodynamics*. Elsevier.
3. BROGLIA, R., ZAGHI, S. and DI MASCIO, A. (2011) '*Numerical simulation of interference effects for a high-speed catamaran'*, Journal of marine science and technology, 16(3), pp. 254–269.
4. CAKICI, F., SUKAS, O. F., KINACI, O. K. and ALKAN, A. D. (2017) '*Prediction of the vertical motions of the dtmb 5415 ship using different numerical approaches*', Brodogradnja, 68(2), pp. 29–44. doi: 10.21278/brod68203.
5. CARRICA, P. M., CASTRO, A. M. and STERN, F. (2010) '*Self-propulsion computations using a speed controller and a discretized propeller with dynamic overset grids'*, Journal of Marine Science and Technology, 15(4), pp. 316–330. doi: 10.1007/s00773-010-0098-6.
6. CASTRO, A. M., CARRICA, P. M. and STERN, F. (2011) '*Full scale self-propulsion computations using discretized propeller for the KRISO container ship KCS*', Computers & Fluids, 51(1), pp. 35–47. doi: 10.1016/j.compfluid.2011.07.005.
7. CD-adapco, S. (2017) 'STAR CCM+ User Guide Version 12.04', *CD-Adapco: New York, NY, USA*.
8. CELIK, I. B., GHIA, U., ROACHE, P. J., FREITAS, C. J., COLEMAN, H. and RAAD, P. E. (2008) '*Procedure for Estimation and Reporting of Uncertainty Due to Discretization in CFD Applications*', Journal of Fluids Engineering, 130(7), pp. 78001–78004. doi: 10.1115/1.2960953.
9. DELEN, C. and BAL, S. (2015a) '*Uncertainty Analysis of Resistance Tests in Ata Nutku Ship Model Testing Laboratory of Istanbul Technical University*', in Towards Green Marine Technology and Transport - Proceedings of the 16th International Congress of the International Maritime Association of the Mediterranean, IMAM 2015.
10. DELEN, C. and BAL, S. (2015b) '*Uncertainty Analysis of Resistance Tests in Ata Nutku Ship Model Testing Laboratory of Istanbul Technical University*', Journal of Maritime and Marine Sciences, 1(2 (2015)), pp. 8–27.
11. DELEN, C., SEZEN, S. and BAL, S. (2017) '*Computational Investigation of Self Propulsion Performance of Darpa Suboff Vehicle*', Tamap Journal of Engineering, 2017(4).
12. DOGRUL, A., SEZEN, S., DELEN, C. and BAL, S. (2017) '*Self-propulsion simulation of DARPA Suboff*', The International Maritime Association of the Mediterranean (IMAM 2017). Edited by C. G. Soares. Lisbon, Portugal.
13. GAGGERO, S., VILLA, D. and VIVIANI, M. (2017) '*An extensive analysis of numerical ship self-propulsion prediction via a coupled BEM/RANS approach'*, Applied Ocean Research, 66, pp. 55–78. doi: https://doi.org/10.1016/j.apor.2017.05.005.
14. GAGGERO, S., VILLA, D. and VIVIANI,, M. (2015) '*The Kriso Container Ship (Kcs) Test Case: An Open Source Overview*', VI International Conference on Computational Methods in Marine Engineering (MARINE 2015). Edited by F. Salvatore and R. Muscari. Rome, Italy.
15. GARCÍA-GÓMEZ, A. (2000) '*On the form factor scale effect*', Ocean Engineering, 27(1), pp. 97–109. Available at: https://ac.els-cdn.com/S0029801898000420/1-s2.0-S0029801898000420-main.pdf?_tid=d99f2015-23e2-46f3-8c07-7496a5816544&acdnat=1546948873_821d7d83f9495b43878f39cc5e851168.
16. GOKCE, M. K., KINACI, O. K. and ALKAN, A. D. (2018) '*Self-propulsion estimations for a bulk carrier*', Ships and Offshore Structures, pp. 1–8.
17. HAASE, M., ZURCHER, K., DAVIDSON, G., BINNS, J. R., THOMAS, G. and BOSE, N. (2016) '*Novel CFD-based full-scale resistance prediction for large medium-speed catamarans*', Ocean Engineering, 111, pp. 198–208. doi: 10.1016/j.oceaneng.2015.10.018.
18. ITTC (2002a) *Recommended Procedures and Guidelines - Resistance Test - 7.5-02-02-0*.
19. ITTC (2002b) '*Testing and Extrapolation Methods Resistance Uncertainty Analysis, Example for Resistance Test*', in.
20. ITTC (2011a) '*1978 ITTC Performance Prediction Method - 7.5 – 02-03 – 01.4*', in International Towing Tank Conference.
21. ITTC (2011b) '*Recommended Procedures and Guidelines - Practical guidelines for ship CFD applications - 7.5-03-02-03*', in International Towing Tank Conference.
22. ITTC (2011c) '*Recommended Procedures and Guidelines - Resistance Test - 7.5-02-02-01*', in

International Towing Tank Conference.
23. ITTC (2011d) '*Recommended Procedures and Guidelines - Ship Models -7.5-01-01-01*', in International Towing Tank Conference.
24. ITTC (2014a) '*Example for Uncertainty Analysis of Resistance Tests in Towing Tanks - 7.5-02-02-02.1*', in International Towing Tank Conference.
25. ITTC (2014b) *Practical Guide for Uncertainty Analysis of Resistance Measurement in Routine Tests - 7.5-02-02-02.2*.
26. ITTC (2014c) '*Recommended Procedures and Guidelines- Practical Guidelines for RANS Calculation of Nominal Wakes -7.5-03-03-02*', in International Towing Tank Conference.
27. JASAK, H., VUKČEVIĆ, V., GATIN, I. and LALOVIĆ, I. (2018) '*CFD validation and grid sensitivity studies of full scale ship self propulsion*', International Journal of Naval Architecture and Ocean Engineering.
28. JONES, A. C. and LAUNDER, D. B. (1972) '*Lectures in mathematical models of turbulence*'. London: Academic Press.
29. KIM, W. J., VAN, S. H. and KIM, D. H. (2001) '*Measurement of flows around modern commercial ship models*', Experiments in fluids, 31(5), pp. 567–578.
30. KINACI, O. K., GOKCE, M. K., ALKAN, A. D. and KUKNER, A. (2018) '*On self-propulsion assessment of marine vehicles*', Brodogradnja: Teorija i praksa brodogradnje i pomorske tehnike, 69(4), pp. 29–51.
31. KINACI, O. K., SUKAS, O. F. and BAL, S. (2016) '*Prediction of wave resistance by a Reynolds-averaged Navier-Stokes equation-based computational fluid dynamics approach*', Proceedings of the Institution of Mechanical Engineers Part M: Journal of Engineering for the Maritime Environment. doi: 10.1177/1475090215599180.
32. KOUH, J.-S., CHEN, Y.-J. and CHAU, S.-W. (2009) '*Numerical study on scale effect of form factor*', Ocean Engineering, 36(5), pp. 403–413. doi: 10.1016/j.oceaneng.2009.01.011.
33. LARSSON, L., STERN, F., VISONNEAU, M., HINO, T., HIRATA, N. and KIM, J. (2018) '*Tokyo 2015: A workshop on CFD in ship hydrodynamics*', in Workshop Proceedings, Tokyo, Dec, pp. 2–4.
34. LARSSON, L., STERN, F. and VISONNEAU, M. (2013) *Numerical ship hydrodynamics: an assessment of the Gothenburg 2010 workshop*. Springer.
35. LIN, T. Y. and KOUH, J. S. (2015) '*On the scale effect of thrust deduction in a judicious self-propulsion procedure for a moderate-speed containership*', Journal of Marine Science and Technology (Japan). Springer Japan, 20(2), pp. 373–391. doi: 10.1007/s00773-014-0289-7.
36. DE LUCA, F., MANCINI, S., MIRANDA, S. and PENSA, C. (2016) '*An Extended Verification and Validation Study of CFD Simulations for Planing Hulls*', Journal of Ship Research, 60(2), pp. 101–118. doi: 10.5957/josr.60.2.160010.
37. DE MARCO, A., MANCINI, S., MIRANDA, S., SCOGNAMIGLIO, R. and VITIELLO, L. (2017) '*Experimental and numerical hydrodynamic analysis of a stepped planing hull*', Applied Ocean Research. Elsevier B.V., 64(March), pp. 135–154. doi: 10.1016/j.apor.2017.02.004.
38. MOLLAND, A. F., TURNOCK, S. R. and HUDSON, D. A. (2011) *Ship resistance and propulsion: Practical estimation of ship propulsive power*, *Ship Resistance and Propulsion: Practical Estimation of Ship Propulsive Power*. doi: 10.1017/CBO9780511974113.
39. NOCEDAL, J. and WRIGHT, S. (2006) *Numerical optimization*. Second Ed. USA: Springer Science & Business Media.
40. OZDEMIR, Y. H., DOGRUL, A., BARLAS, B. and COSGUN, T. (2016) '*A Numerical Application to Predict the Resistance and Wave Pattern of Kriso Container Ship*', Brodogradnja, 67(2), pp. 47–65. doi: 10.21278/brod67204.
41. PARK, S., OH, G., HYUNG RHEE, S., KOO, B.-Y. and LEE, H. (2015) '*Full scale wake prediction of an energy saving device by using computational fluid dynamics*', Ocean Engineering, 101(Supplement C), pp. 254–263. doi: https://doi.org/10.1016/j.oceaneng.2015.04.005.
42. QUÉRARD, A., TEMAREL, P. and TURNOCK, S. R. (2008) '*Influence of viscous effects on the hydrodynamics of ship-like sections undergoing symmetric and anti-symmetric motions, using RANS*', in ASME 2008 27th International Conference on Offshore Mechanics and Arctic Engineering. American Society of Mechanical Engineers, pp. 683–692.
43. RINA (1977) 'The Transaction of The Royal Institution of Naval Architects', 119, pp. lxvi–lxvii.
44. SEZEN, S., DOGRUL, A., DELEN, C. and BAL, S. (2018) '*Investigation of self-propulsion of DARPA Suboff by RANS method*', Ocean Engineering. Elsevier Ltd, 150(November 2017), pp. 258–271. doi: 10.1016/j.oceaneng.2017.12.051.
45. SHEN, Z., WAN, D. and CARRICA, P. M. (2015) '*Dynamic overset grids in OpenFOAM with application to KCS self-propulsion and maneuvering*', Ocean Engineering, 108, pp. 287–306. doi: 10.1016/j.oceaneng.2015.07.035.
46. SIMONSEN, C. D., OTZEN, J. F., JONCQUEZ, S. and STERN, F. (2013) '*EFD and CFD for KCS heaving and pitching in regular head waves*', Journal of Marine Science and Technology, 18(4), pp. 435–459. doi: 10.1007/s00773-013-0219-0.
47. SONG, S., DEMIREL, Y. K. and ATLAR, M. (2019) '*An investigation into the effect of*

biofouling on the ship hydrodynamic characteristics using CFD', Ocean Engineering. Elsevier, 175, pp. 122–137.

48. SRINAKAEW, S. (2017) *A numerical study of resistance components of high-speed catamarans and the scale effects on form factor*.
49. STERN, F., WILSON, R. V., COLEMAN, H. W. and PATERSON, E. G. (2002) '*Comprehensive Approach to Verification and Validation of CFD Simulations* Part 1: Methodology and Procedures', Journal of Fluids Engineering, 123(4), p. 793. doi: 10.1115/1.1412235.
50. TELFER, E. V (1927) '*Ship resistance similarity*', Trans. *INA*, 69.
51. TERZIEV, M., TEZDOGAN, T., OGUZ, E., GOURLAY, T., DEMIREL, Y. K. and INCECIK, A. (2018) '*Numerical investigation of the behaviour and performance of ships advancing through restricted shallow waters*', Journal of Fluids and Structures. Academic Press, 76, pp. 185–215. doi: 10.1016/J.JFLUIDSTRUCTS.2017.10.003.
52. TEZDOGAN, T., DEMIREL, Y. K., KELLETT, P., KHORASANCHI, M., INCECIK, A. and TURAN, O. (2015) '*Full-scale unsteady RANS CFD simulations of ship behaviour and performance in head seas due to slow steaming*', Ocean Engineering, 97, pp. 186–206. doi: 10.1016/j.oceaneng.2015.01.011.
53. TEZDOGAN, T., INCECIK, A. and TURAN, O. (2016) '*Full-scale unsteady RANS simulations of vertical ship motions in shallow water*', Ocean Engineering, 123, pp. 131–145. doi: 10.1016/j.oceaneng.2016.06.047.
54. USTA, O. and KORKUT, E. (2018) '*A study for cavitating flow analysis using DES model*', Ocean Engineering. Elsevier, 160, pp. 397–411.
55. VAN, S. H., KIM, W. J., YIM, G. T., KIM, D. H. and LEE, C. J. (1998) '*Experimental Investigation of the Flow Characteristics around Practical Hull Forms*', in 3rd Osaka Colloquium on Advanced CFD Applications to Ship Flow and Hull Form Design, pp. 215–227.
56. WALKER, F. M. (2010) *Ships and shipbuilders: Pioneers of design and construction*. Seaforth Publishing.
57. WANG, Z.-Z., XIONG, Y., WANG, R., SHEN, X.-R. and ZHONG, C.-H. (2015) '*Numerical study on scale effect of nominal wake of single screw ship*', Ocean Engineering, 104, pp. 437–451. doi: https://doi.org/10.1016/j.oceaneng.2015.05.029.

